Energy Proceedings
Vol 39, 2024
ISSN 2004-2965

Hemispherical Emittance in Multilayer Solar Absorbers: A MATLAB-Based Approach for Optimizing Solar Thermal Efficiency

Eliana Gaudino[1,2], Antonio Caldarelli[2], Daniela De luca[2], Umar Farooq[2,3], Paolo Strazzullo[1,2], Emiliano Di Gennaro[2,3], Marilena Musto[1,2], Roberto Russo[2*]

1 Industrial Engineering Department, University of Napoli "Federico II", Piazzale Vincenzo Tecchio, 80, 80125 Napoli, Italy
2 Institute of Applied Sciences and Intelligent Systems, National Research Council of Italy, via Pietro Castellino 111 80131 Napoli,Italy
3 Physics Department, University of Napoli "Federico II", Via Cinthia, 21, Napoli, 80126, Italy

ABSTRACT

The thermal emissivity of selective solar absorbers is a critical determinant of their operational efficiency. This paper details the computation of hemispherical emissivity for multi-layered coatings, specifically designed and optimized for solar thermal applications, particularly within high vacuum flat collectors at temperatures up to 200°C. We employed a MATLAB script, underpinned by the transfer matrix method, to calculate the hemispherical emissivity. The calculated emissivity values aligned well with experimental measurements derived from sputter-deposited samples. Our findings underscore the efficacy of the designed multi-layered coatings in relation to their thermal emissivity characteristics, thus highlighting their potential for solar thermal applications.

Keywords: solar thermal, solar energy, solar absorbers, multilayer coatings characterization, evacuated solar thermal collectors

NOMENCLATURE

Abbreviations	
abs	Absorber
hem	Hemispherical
HVFPC	High Vacuum Flat Plate Collector
OTL	Other Thermal Losses
Low-e	Low emissivity
ms	measured
MTB	Mini Test Box
nl	numerical
sub	Substrate
SSA	Selective Solar Absorber
Symbols	
α	Spectrally averaged absorptance
ε	Spectrally averaged emissivity
λ	Wavelength
σ	Stefan-Boltzmann constant W/m^2K^4
θ	Angle of emission
τ	Transmittance

1. INTRODUCTION

Heat is a critical component in various industrial processes, and the need for heat production is essential for many industries. Currently, industrial heat production is largely satisfied through fossil fuel combustion, a significant contributor to greenhouse gas emissions and climate change [1]. As the world moves towards a more sustainable and low-carbon future, there is a growing need to transition towards cleaner and more efficient heat production methods. One possible solution lies in the utilization of renewable energy sources such as solar thermal energy [2]. Selective solar absorbers (SSAs) are a critical component of solar energy harvesting systems, as they enable the absorption of solar radiation and conversion into thermal energy with higher efficiency than traditional absorbers [3]. These materials are designed to selectively absorb solar radiation in the desired wavelength range while minimizing thermal radiation losses from their surface. This selective absorption is achieved by tailoring the optical and thermal properties of the material, typically through the use of multilayer coatings or nanostructured surfaces [4]. Low-emissivity (low-e) multilayer coatings are among the most promising methods to achieve selective absorption in solar absorbers. These coatings are designed to reduce thermal radiation losses from the surface while still maintaining high solar absorbance [5]. This is typically achieved by using a stack of thin film layers with alternating high and low refractive indices, which create interference effects that selectively enhance or suppress the reflection and transmission of light at specific wavelengths. The resulting multilayer coating can have a high solar absorptance and a low hemispherical emittance, leading to high thermal

This is a paper for 15th International Conference on Applied Energy (ICAE2023), Dec. 3-7, 2023, Doha, Qatar.

efficiency [6]. SSAs have a wide range of applications, and one of the most promising is steam production with highly efficient solar thermal collectors such as evacuated collectors [7].In fact, since radiative heat losses are the only cause of efficiency reduction for this type of collector, optimizing the optical absorber parameters, particularly the thermal emittance, is crucial In reference [8], the development of optimized low-e multilayer coatings for unconcentrated thermal applications is discussed. The optimization of the thickness layers was performed using a genetic algorithm based on the transfer matrix method [9] that maximizes the absorbers' efficiency at the chosen optimization temperature. In the calculation of the absorber efficiency it was considered the directional thermal emittance at an angle of 0° but, in the context of solar absorbers, the directional emittance $\varepsilon_{\theta}(T)$ is the critical parameter to consider when designing and optimizing the absorber for concentrated solar power systems [10]. These systems require the absorber to efficiently radiate thermal energy towards the receiver, typically positioned above the absorber [11]. For innovative high vacuum flat plate collectors, the parameter to consider for the optimization is the hemispherical emittance $\varepsilon_{he}\ (T)$ [12] because the absorber surface can emit thermal radiation in all directions from both surfaces. Accurate models of the collector performance require an understanding of the absorber's emittance in all directions $\varepsilon_{hem}(T)$, as this affects the amount of energy that is emitted by the collector. The value of $\varepsilon_{hem}(T)$, in fact, a direct impact on the computation of the heat losses, the thermal efficiency of the collector at a certain operating temperature and, ultimately, its annual producibility.

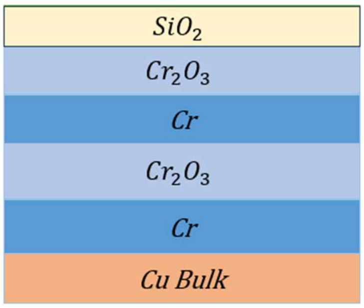

Fig. 1 . Architecture of the analyzed multilayer coating.

In this work, the hemispherical emittance of an SSA composed of a copper substrate coated with a Cr-Cr_2O_3-SiO_2 multilayer (fig.1), optimized to work at temperature of 200 °C in high vacuum flat plate collectors, is computed using a MATLAB script based on the transfer matrix method. The computed emittance was compared with experimental measurements performed with a dedicated experimental set-up [13].

2. METHODS

2.1 Optimized SSA hemispherical emittance calculation

The most general definition of emissivity is the ratio of the energy radiated from a material's surface to that radiated from a blackbody, at identical temperature and wavelength and under the same viewing conditions. The spectral directional emissivity $\varepsilon_{\lambda-\theta}(T)$, describes emissivity at specific wavelengths and directions and it depends by factors such as material composition, surface oxidation, and surface temperature. By integrating $\varepsilon_{\lambda-\theta}$, in all directions and wavelengths, the total hemispherical emittance $\varepsilon_{hem}(T)$ can be obtained. The numerical model used in a MATLAB script to compute hemispherical emissivity of multilayer utilizes Kirchoff's law which relates the spectral and directional emissivity to reflectance [14]. This is computed with the transfer matrix method [9] and optical constants of the material [15]. The model requires as first step to define the layers of the multilayer stack and their respective thicknesses, refractive indices, and extinction coefficients, then using the properties of each layer, a transfer matrix for each layer that describes the reflection and transmission of electromagnetic waves at the interfaces between the layers can be constructed. Multiplying the transfer matrices for each layer to obtain the overall transfer matrix for the multilayer stack, which describes the reflection and transmission of electromagnetic waves through the entire stack. From the overall transfer matrix, it is possible to compute the reflectance and transmittance of the multilayer stack for a given wavelength and direction. Once obtained $\varepsilon_{\lambda-\theta}(T)$ applicating the Kirkoff's law, $\varepsilon_{\lambda}(T)$ is obtainable integrating in all angles as showed in eq. (1):

$$\varepsilon_{\lambda}(T) = 2\int_{0}^{\pi/2} \varepsilon_{\lambda-\theta}(T)\, sin(\vartheta) cos(\vartheta) \delta\vartheta \qquad (1)$$

For the integrations was used the rectangular rule described in [15]. The total hemispherical emissivity is obtained from a further integration over the Planck distribution via (2):

$$\varepsilon(T) = \frac{\int_{0}^{\propto} \varepsilon_{\lambda}(T) B(\lambda,T) \delta\lambda}{\sigma T^4} \qquad (2)$$

Where $B(\lambda, T)$ is the blackbody emissive power at temperature T.

In this first stage of computation, the effect of surface roughness on the total hemispherical emittance was neglected.

2.2 Optimized SSA hemispherical emittance experimental measurements

To validate the numerical model, the calculated total hemispherical emittance values were compared with that obtained with experimental measurements performed on sputter- deposited SSA small samples (Area= 100 cm^2). The multilayer coating of the solar absorber was developed and optimized for a specific application that is middle temperature steam generation using high vacuum flat plate collectors (HVFPCs), for this reason, an experimental set- up that reproduces faithfully an HVFPC, named Mini Test Box (MTB), was developed in order to measure radiative properties of the SSA samples. The MTB system, shown in Fig.2 and described in detail in [13].

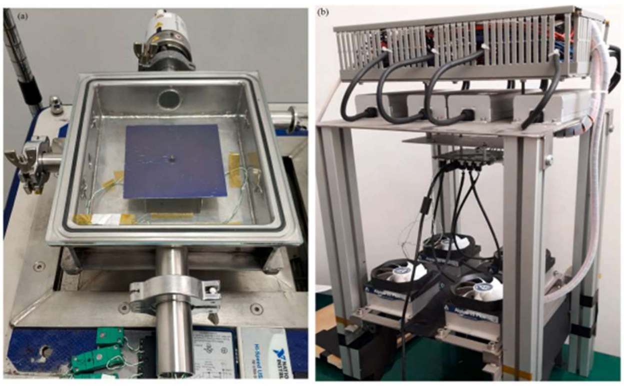

Fig. 2 (a) The mini-test box system apparatus; (b) LED array system

The hemispherical emittance of the SSA can be determined through a calorimetric approach. Eq. (3) represents a power balance equation that takes into account the radiative exchanges between absorber (frontside) and glass and absorber (substrate, back side) and vessel and the other thermal losses (OTL) imputable on the conduction of small components of the experimental set up in contact with the absorber (support springs, thermocouple bolt, etc…):

$$m_{abs} c_p(T_{abs}) \frac{dT_{abs}}{dt} = \alpha\ A\ \tau\ P_{in} - \varepsilon'_{abs}(T_{abs})\sigma\ A\ (T_a^4 - T_g^4) - \varepsilon'_{sub}(T_{sub})\sigma\ A\ (T_{abs}^4 - T_v^4) - OTL(T_{abs}) \quad (3)$$

where the parameters m_{abs}, c_p, T_{abs}, α and A represent the selective solar absorber mass, specific heat capacity, temperature, absorptance, and area; ε'_{abs} (T_{abs}) is the absorber equivalent thermal emittance, between glass and absorber ε'_{abs} (T_{abs}) = $\left(\frac{1}{\frac{1}{\varepsilon_{glass}}+\frac{1}{\varepsilon_{abs}}-1}\right)$; τ describes the glass transmittance, P_{in} the incident radiation per unit of area; T_g is the glass temperature; T_v is the vessel temperature and ε'_{sub} (T_{sub}) is the substrate equivalent thermal emittance between stainless steel envelope and substrate $\varepsilon'_{sub}(T_{sub}) = \left(\frac{1}{\frac{1}{\varepsilon_{steel}}+\frac{1}{\varepsilon_{sub}}-1}\right)$.

The term OTL has been experimentally evaluated as function of the temperature and they will be reported in a separate paper.

During the measurements, the negligible recorded variation (within a few degrees) between the two sets of data on T_g and T_v allows to simplify Eq. (3) as follows:

$$m_{abs} c_p(T_{abs}) \frac{dT_{abs}}{dt} = \alpha\ A\ \tau\ P_{in} - \varepsilon_{tot}(T_{abs})\sigma\ A\ (T_a^4 - T_m^4) - OTL(T_{abs}) \quad (4)$$

where ε_{tot} (T_{amb}) is the sum of ε'_{abs}(T_{abs}) and ε'_{sub}(T_{sub}) and T_m is the average between T_g and T_v. The parameter ε_{tot} in Eq. (4), is the hemispherical emittance objective of the measurements. The temperature T_{abs} of the sample under analysis is increased until the achievement of stagnation temperature by LED array illumination and subsequently cooled turning off the illumination. During the cooling down phase (when P_{in} = 0), ε_{tot} (T_{abs}) can be evaluated as it remains the only unknown quantity because all the other variables present in eq. (4) are known or measured by sensors installed on the MTB.

3. RESULTS AND DISCUSSION

Figure 3 presents experimental results of the hemispherical emittance as a function of absorber temperature for the optimized multilayer structure depicted in Figure 1. Additionally, the figure displays both the hemispherical and directional (θ =0) emittances

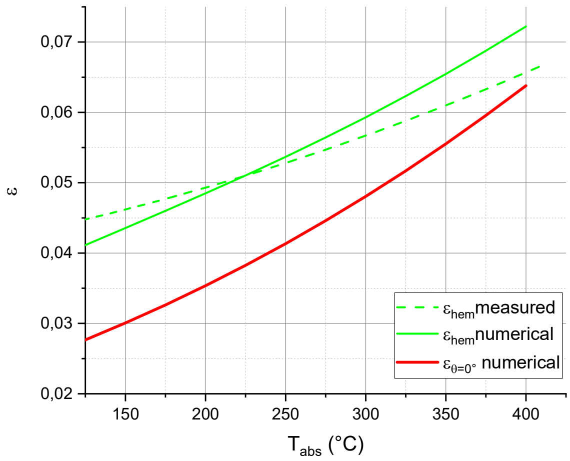

Fig.3 measured hemispherical (dashed green line), numerical hemispherical (solid green line) and numerical directional (solid red line) emittance curves of the optimized SSA computed using a MATLAB script based on the model described in Section 2.1.

The refractive indices of the constituent materials of the multilayer stack, which are essential inputs to the numerical model, were determined in the 300-1600 nm range using a Jobin Yvon Horiba phase-modulated spectrophotometer.

As expected the computed directional emittance at an angle of (θ =0) is not a suitable to calculate the thermal losses, as it yields a value of $\varepsilon_{\theta=0}(200\ °C) = 0.035$, which deviates by approximately 29% from the measured value of the hemispherical emittance, $\varepsilon_{\text{hem ms}}(200\ °C) = 0.049$. In contrast, the computed hemispherical emittance at the optimization temperature is, exhibiting a deviation of only 2% from the experimental value. The trend of the computed hemispherical emittance $\varepsilon_{\text{hem\_nl}}(200\ °C) = 0.048$ is generally consistent with the experimental measurements, suggesting that the approximation made in the numerical model is accurate.

4. CONCLUSIONS

The study conducted measurements and computations of the hemispherical emittance of low-e Selective Solar Absorbers designed for use in middle-temperature industrial applications (200 °C). These calculations were performed using a MATLAB numerical code based on the transfer matrix method, and were found to be consistent with experimental measurements, thereby validating the numerical model.

Furthermore, the study compared the numerical results with the computed directional emittance at (θ =0), which was used as a parameter in the optimization algorithm for determining the thickness of each layer of the low-e SSA. However, the comparison revealed that the correct optimization parameter for designing and optimizing SSAs is the hemispherical emittance. Therefore, the optimization algorithm should include the calculation of hemispherical emittance for future optimizations. This result is essential to correctly compute the thermal radiative losses in HVFPC and their daily and yearly energy production.

REFERENCES

[1] W. Puntoon, P. Tarkhamtham, e R. Tansuchat, «The impacts of economic growth, industrial production, and energy consumption on CO2 emissions: A case study of leading CO2 emitting countries», *Energy Reports*, vol. 8, pp. 414–419, dic. 2022, doi: 10.1016/j.egyr.2022.10.219.

[2] M. I. Ismail, N. A. Yunus, e H. Hashim, «Integration of solar heating systems for low-temperature heat demand in food processing industry – A review», *Renewable and Sustainable Energy Reviews*, vol. 147, p. 111192, set. 2021, doi: 10.1016/j.rser.2021.111192.

[3] F. Cao, K. McEnaney, G. Chen, e Z. Ren, «A review of cermet-based spectrally selective solar absorbers», *Energy Environ. Sci.*, vol. 7, fasc. 5, p. 1615, 2014, doi: 10.1039/c3ee43825b.

[4] A. Dan e B. Basu, «Understanding spectrally selective properties of solar absorbers», in *Energy Saving Coating Materials*, Elsevier, 2020, pp. 133–151. doi: 10.1016/B978-0-12-822103-7.00006-6.

[5] A. Caldarelli *et al.*, «Low emissivity thin film coating to enhance the thermal conversion efficiency of selective solar absorber in high vacuum flat plate collectors», *Thin Solid Films*, vol. 764, p. 139632, gen. 2023, doi: 10.1016/j.tsf.2022.139632.

[6] D. De Maio *et al.*, «Multilayers for efficient thermal energy conversion in high vacuum flat solar thermal panels», *Thin Solid Films*, vol. 735, p. 138869, ott. 2021, doi: 10.1016/j.tsf.2021.138869.

[7] D. Gao, J. Li, X. Ren, T. Hu, e G. Pei, «A novel direct steam generation system based on the high-vacuum insulated flat plate solar collector», *Renewable Energy*, vol. 197, pp. 966–977, set. 2022, doi: 10.1016/j.renene.2022.07.102.

[8] D. De Maio, C. D'Alessandro, A. Caldarelli, M. Musto, e R. Russo, «Solar selective coatings for evacuated flat plate collectors: Optimisation and efficiency robustness analysis», *Solar Energy Materials and Solar Cells*, vol. 242, p. 111749, ago. 2022, doi: 10.1016/j.solmat.2022.111749.

[9] M. Huang, F. Cegla, e B. Lan, «Stiffness matrix method for modelling wave propagation in arbitrary multilayers», *International Journal of Engineering Science*, vol. 190, p. 103888, set. 2023, doi: 10.1016/j.ijengsci.2023.103888.

[10] V. Pranesh, R. Velraj, S. Christopher, e V. Kumaresan, «A 50 year review of basic and applied research in compound parabolic concentrating solar thermal collector for domestic and industrial applications», *Solar Energy*, vol. 187, pp. 293–340, lug. 2019, doi: 10.1016/j.solener.2019.04.056.

[11] M. J. Blanco, J. G. Martín, e D. C. Alarcón-Padilla, «Theoretical efficiencies of angular-selective non-concentrating solar thermal systems», *Solar Energy*, vol. 76, fasc. 6, pp. 683–691, 2004, doi: 10.1016/j.solener.2004.01.005.

[12] L. Granados, S. Huang, D. R. McKenzie, e A. W. Y. Ho-Baillie, «The importance of total hemispherical emittance in evaluating performance of building-

integrated silicon and perovskite solar cells in insulated glazings», *Applied Energy*, vol. 276, p. 115490, ott. 2020, doi: 10.1016/j.apenergy.2020.115490.

[13] C. D'Alessandro *et al.*, «Calorimetric testing of solar thermal absorbers for high vacuum flat panels», *Solar Energy*, vol. 243, pp. 81–90, set. 2022, doi: 10.1016/j.solener.2022.07.039.

[14] R. G. Hering e T. F. Smith, «Surface radiation properties from electromagnetic theory», *International Journal of Heat and Mass Transfer*, vol. 11, fasc. 10, pp. 1567–1571, ott. 1968, doi: 10.1016/0017-9310(68)90117-8.

[15] J. L. King, H. Jo, S. K. Loyalka, R. V. Tompson, e K. Sridharan, «Computation of total hemispherical emissivity from directional spectral models», *International Journal of Heat and Mass Transfer*, vol. 109, pp. 894–906, giu. 2017, doi: 10.1016/j.ijheatmasstransfer.2017.01.120.